

A model of non-Gaussian intracellular diffusion

Yann Lanoiselée

E-mail: yann.lanoiselee@polytechnique.edu
Laboratoire de Physique de la Matière Condensée (UMR 7643),
CNRS – Ecole Polytechnique, University Paris-Saclay, 91128 Palaiseau, France

Denis S. Grebenkov

E-mail: denis.grebenkov@polytechnique.edu
Laboratoire de Physique de la Matière Condensée,
CNRS – Ecole Polytechnique, F-91128 Palaiseau, France
Interdisciplinary Scientific Center Poncelet (ISCP),[‡]
Bolshoy Vlas'yevskiy Pereulok 11, 119002 Moscow, Russia

Abstract. Recent progresses in single particle tracking have shown evidences of non-Gaussian distribution of displacements in living cells, both near the cellular membrane and inside the cytoskeleton. A similar behavior has also been observed in granular media, turbulent flows, gels, and colloidal suspensions, suggesting that this is a general feature of diffusion in complex media. A possible interpretation of this phenomenon is that a tracer explores a medium with spatio-temporal fluctuations which result in local changes of diffusivity. We propose and investigate an ergodic, easily interpretable model, which implements the concept of diffusing diffusivity. Depending on the parameters, the distribution of displacements can be either flat or peaked at small displacements with an exponential tail at large displacements. We show that the distribution converges slowly to a Gaussian one. We calculate statistical properties, derive the asymptotic behavior, and discuss some implications and extensions.

Keywords: non-Gaussian diffusion, diffusing diffusivity, intracellular transport, superstatistics

PACS numbers: 02.50.-r, 05.60.-k, 05.10.-a, 02.70.Rr

[‡] International Joint Research Unit – UMI 2615 CNRS/ IUM/ IITP RAS/ Steklov MI RAS/ Skoltech/ HSE, Moscow, Russian Federation

1. Introduction

A reliable description of transport processes in complex media, such as living cells, is a challenging problem. The primary biological motivation is to understand how the intracellular transport can be efficient enough to allow cell life in crowded environments. From the physical perspective, the challenge stands in elaborating a unified mesoscopic description of transport in disordered media which is consistent with experimental observations of single particle trajectories.

The past years witnessed numerous experimental observations of anomalous diffusion with the Mean Squared Displacement (MSD) evolving as a power law $\langle X^2(t) \rangle \propto t^\alpha$ [1, 2, 3, 4, 5]. Many models have been proposed to rationalize this power law [6, 7, 8], each model providing a different interpretation of the effect of crowding on tracer's motion in the subdiffusive case $\alpha < 1$. The anomalous scaling can originate from (i) diffusion in a fractal medium due to the excluded volume; (ii) viscoelastic properties of the medium described by fractional Brownian motion [9] or generalized Langevin equation [10, 11, 12]; (iii) molecular caging when the tracer is stopped for a random power law distributed time described by Continuous Time Random Walk [13, 14]. Having very different physical origins, these models presuppose that dynamic properties of the medium are homogeneous.

Additionally to the anomalous scaling, recent progress in single particle tracking techniques led to the discovery of a class of systems in which individual particles exhibit non-Gaussian diffusion with exponential tails. This interesting feature is not exclusive to microbiology but has appeared in various complex media. Three typical shapes of distribution of displacements have been observed: (i) flat distribution near zero with an exponential tail is found in granular materials [15], turbulent flow [16], cytoskeleton [17], active gels [18, 19, 20], glassy material [21] and intracellular medium [22], (ii) exponential behavior in entangled F-actin networks [23, 24], log-return of stock prices [25], and (iii) stretched exponential form in granular gas [26], cell membrane [27] and in crowded environments [28, 29]. A common feature of these dynamics is that the displacement distribution becomes Gaussian in the long-time limit [30].

The abundance of empirical observations suggests that exponential tails are reminiscent of heterogeneous complex media despite different experimental and microscopic setups. Aiming at modeling these exponential tails, we proceed by a mesoscopic approach, which describes the system with time-dependent macroscopic quantities. In this article we focus on the case when non-Gaussian diffusion originates from local changes in diffusive properties of the medium. Former contributions from the theoretical side started with the Kärger model [31, 32] in which a particle randomly switches between a finite number of states with different diffusivities. Chubynsky and Slater [33] modeled diffusivity as a continuous random process with a stationary distribution, and deduced from it the short-time exponential behavior [23] using superstatistical description [34, 35]. Jain and Sebastian solved the time-dependent problem in the case when diffusivity is the square of a multidimensional Ornstein-Uhlenbeck process and

showed that it can be mapped to a first passage problem in a medium with absorbing sinks [36, 37]. They also generalized the solution to the case of Lévy driven noise [38]. Chechkin *et al.* [39] solved the problem using subordination technique and pointed out that superstatistical description matches diffusing diffusivity but only at short times as it cannot reproduce convergence to a Gaussian distribution at long times.

We present a three parameter model of non-Gaussian diffusion in which diffusivity is fluctuating around an average value \bar{D} (m^2/s) (which constitutes the effective diffusion coefficient at long time), with the correlation time τ (s) and the amplitude of fluctuations σ (m/s). The description is formulated in terms of coupled Langevin equations from which the characteristic function of displacements is derived in an exact explicit form. The shape of the distribution is tuned by one dimensionless parameter

$$\nu = \frac{\bar{D}}{\sigma^2\tau}, \quad (1)$$

which compares the diffusivity correlation time τ and the diffusivity fluctuation time \bar{D}/σ^2 . Depending on ν , the distribution of displacements can be close to exponential ($\nu = 1$), parabolic ($\nu > 1$) or peaked at the origin ($\nu < 1$). In all cases the distribution of displacement exhibits an exponential tail with eventual power law corrections. We show that this description leads to a linear dependence of the MSD on time, while fluctuations of time-averaged MSD span up at long times depicting the effect of heterogeneous diffusivity. We analyze the autocorrelation of squared increments which describes memory loss of diffusivity. These correlations lead to slow, $1/t$, convergence of the distribution to a Gaussian one. Analytical results are verified numerically by Monte Carlo simulations using Milstein scheme [40]. Finally we derive the asymptotic behavior and discuss some implications and generalizations.

2. Model of non-Gaussian diffusion

We propose a model of a tracer motion in a heterogeneous medium, in which the diffusivity is a stochastic process instead of being a constant. In order to justify this description, let us consider a single particle tracking measurement of duration t_{exp} with a timestep Δt between two position recording. If the motion occurs in a homogeneous environment, the distribution of displacements becomes Gaussian very fast, in a time t_{loc} of equilibration of the tracer with its local environment. For a heterogeneous medium, in which the diffusivity can vary spatio-temporally (noted $D_{x,t}$), we introduce the time t_{sys} for a particle to explore the whole medium and average diffusivities experienced in the medium. On one hand, if $t_{loc} \ll t_{sys} < \Delta t$, increments of the motion are already coarse-grained at a measurement timestep Δt and therefore are Gaussian. On the other hand, if $t_{loc} < \Delta t \ll t_{sys}$, the motion is not Gaussian because diffusivity evolves in time, and the tracer continuously moves from one equilibrium state to another. This can be biologically interpreted as the effect of spatio-temporal heterogeneities in the medium seen from the point of view of a single particle. In general, the diffusivity is

space-time dependent D_{x_t} and locally varying. To simplify the analysis we describe diffusivity as a stochastic process in time D_t , with the idea that the stochasticity is an annealed simplification of the spatio-temporal disorder. The particle experiences a fluctuating diffusivity around an average value \bar{D} toward which the time-averaged effective diffusion coefficient converges at long times (i.e. $t \gg t_{sys}$). Two physical constraints for a fluctuating diffusivity are (i) the distribution of displacements converges to a Gaussian one at long times, so diffusivity should have a stationary distribution in the long-time limit, with the average value \bar{D} ; (ii) diffusivity as a measure of local kinetic energy of the tracer should be non-negative.

We propose to model time-dependent diffusivity D_t as a Cox-Ingersoll-Ross process (CIR) [41], also known as Feller's process or square root process. This process has been developed in order to rationalize fluctuations of volatility in price asset returns. In the CIR model, the diffusivity fluctuates in a harmonic potential centered on \bar{D} and remains non-negative thanks to the balance between the pulling of harmonic potential and the noise reduction of diffusivity-dependent fluctuations at small D_t . Moreover, the stationary distribution of diffusivity is known to be a Gamma distribution. For the sake of clarity, we first formulate the model for one-dimensional motion and then show its straightforward extension to the high-dimensional isotropic case. For a tracer starting at x_0 with diffusivity D_0 , the corresponding coupled Langevin equations read:

$$\begin{cases} dx_t = \sqrt{2D_t}dW_t^{(1)}, \\ dD_t = \frac{1}{\tau}(\bar{D} - D_t)dt + \sigma\sqrt{2D_t}dW_t^{(2)}, \end{cases} \quad (2)$$

where x_t and D_t are stochastic time-dependent position and diffusivity of the tracer, $dW_t^{(1)}$ and $dW_t^{(2)}$ are increments of independent Wiener processes (white noises). The model includes three parameters: the average diffusivity \bar{D} (in m^2/s), the correlation time τ (in s) and the amplitude of fluctuations σ (in m/s).

The approach by Chubynsky and Slater [33] is retrieved by setting a diffusivity bias $s(D) = -\frac{1}{\tau}(D - \bar{D})$ and a diffusivity of diffusivity $d(D) = \sigma^2\sqrt{2D}$, although in our model, reflecting boundaries are not needed. Jain and Sebastian [36] and Chechkin *et al.* [39] considered the diffusivity as the distance from the origin of an n -dimensional Ornstein-Uhlenbeck process, which is a particular case of our model. We present in Appendix A the derivation of the Cox-Ingersoll-Ross model starting from the n -dimensional Ornstein-Uhlenbeck process. It is then evident that previous results can be reproduced for integer values $n = \frac{2\bar{D}}{\sigma^2\tau}$ and the range of applicability is thus widened because parameters in our model are continuous: $\{\tau, \bar{D}, \sigma\} \in (0, \infty)$.

We introduce the propagator $P(x, D, t|x_0, D_0)$, the probability for a tracer to be at x with diffusivity D at time t , when started from x_0, D_0 at $t = 0$. The corresponding forward Fokker-Planck equation reads

$$\frac{\partial}{\partial t}P(x, D, t|x_0, D_0) = \frac{1}{\tau}\frac{\partial}{\partial D}[(D - \bar{D})P] + D\frac{\partial^2}{\partial x^2}P + \sigma^2\frac{\partial^2}{\partial D^2}(DP), \quad (3)$$

with the initial condition $P(x, D, t = 0|x_0, D_0) = \delta(x - x_0)\delta(D - D_0)$.

Following Drăgulescu and Yakovenko [25], this equation is solved by performing the

Fourier transform with respect to position x , and the Laplace transform with respect to diffusivity $D \geq 0$:

$$\tilde{P}(q, s, t|x_0, D_0) = \int_{-\infty}^{\infty} dx \int_0^{\infty} dD e^{-iqx - Ds} P(x, D, t|x_0, D_0), \quad (4)$$

where q and s are the dual variables to position and diffusivity, respectively. Inserting Eq. (4) into Eq. (3) leads to the first order partial differential equation:

$$\frac{\partial}{\partial t} \tilde{P} + \left(\sigma^2 s^2 + \frac{1}{\tau} s - q^2 \right) \frac{\partial}{\partial s} \tilde{P} = -\frac{1}{\tau} \bar{D} s \tilde{P}, \quad (5)$$

subject to the initial condition $\tilde{P}(q, s, t = 0|x_0, D_0) = e^{-iqx_0} e^{-sD_0}$. Its solution is derived in Appendix B

$$\tilde{P}(q, s, t|x_0, D_0) = F(x_0, D_0, s) \left(\frac{\sigma^2}{\Omega} \left(s + \frac{1}{\tau} + \frac{\Omega}{2\sigma^2} \right) (1 - \xi e^{-\Omega t}) e^{\left(\frac{-\frac{1}{\tau} + \Omega}{2} \right) t} \right)^{\frac{-\bar{D}}{\sigma^2 \tau}}, \quad (6)$$

with $F(x_0, D_0, s) = \exp \left[-iqx_0 - D_0 \left(\frac{1}{\sigma^2} + \frac{\Omega}{\sigma^2} \frac{2}{1 - \xi e^{-\Omega t}} \right) \right]$, $\xi = 1 - \frac{2\Omega}{\sigma^2 s + \frac{1}{\tau} + \Omega}$ and $\Omega = \sqrt{\frac{1}{\tau^2} + 4\sigma^2 q^2}$.

The inverse Fourier and Laplace transforms yield $P(x, D, t|x_0, D_0)$. However this solution provides too detailed information which can hardly be confronted to single particle tracking data with no direct access to diffusivities D and D_0 . We thus integrate the solution over D (which is equivalent to set $s = 0$) to get the marginal distribution of positions. We also assume that the tracer's initial diffusivity D_0 is taken from its stationary Gamma distribution $\Pi(D_0)$ (see Appendix B):

$$\Pi(D_0) = \frac{\nu^\nu D_0^{\nu-1}}{\Gamma(\nu) \bar{D}^\nu} \exp \left(-\frac{\nu}{\bar{D}} D_0 \right), \quad (7)$$

where the shape parameter ν is defined in Eq. (1). The average over D_0 yields the marginal distribution

$$P(x, t|x_0) = \frac{1}{2\pi} \int_{-\infty}^{\infty} dq e^{-iqx_0} \tilde{P}(q, t) \quad (8)$$

with

$$\tilde{P}(q, t) = \left(e^{-\frac{1}{2}(\omega-1)t^*} \frac{4\omega}{(\omega+1)^2} \left(1 - \left(\frac{\omega-1}{\omega+1} \right)^2 e^{-\omega t^*} \right)^{-1} \right)^\nu, \quad (9)$$

where we introduced the dimensionless time $t^* = t/\tau$, and $w = \Omega\tau = \sqrt{1 + 4q^2\sigma^2\tau^2}$. An alternative solution using the subordination concept inspired from [39] is given in Appendix C.

When particles undergo isotropic motion in \mathbb{R}^d , the formula for the distribution of displacements remains almost unchanged, except that one has to perform multi-dimensional inverse Fourier transform on the domain \mathbb{R}^d , with \mathbf{q} , \mathbf{x} and \mathbf{x}_0 being vectors:

$$P(\mathbf{x}, t|\mathbf{x}_0) = \int_{\mathbb{R}^d} \frac{d^d \mathbf{q}}{(2\pi)^d} e^{i\mathbf{q}(\mathbf{x}-\mathbf{x}_0)} \tilde{P}(|\mathbf{q}|, t), \quad (10)$$

with $w = \sqrt{1 + 4\sigma^2\tau^2|\mathbf{q}|^2}$. Since the characteristic function $\tilde{P}(|\mathbf{q}|, t)$ depends only on $|\mathbf{q}|$, one can use spherical coordinates and integrate out the angular variables, yielding

$$P(r, t) = \frac{r^{1-d/2}}{(2\pi)^{d/2}} \int_0^\infty dq q^{d/2} J_{\frac{d-2}{2}}(qr) \tilde{P}(q, t), \quad (11)$$

where $J_\alpha(x)$ is the Bessel function of the first kind, $r = |\mathbf{x} - \mathbf{x}_0|$, and $\tilde{P}(q, t)$ is given by Eq. (8). In what follows, we focus on the one-dimensional case, bearing in mind straightforward extensions to the multi-dimensional case.

Figure 1 shows the convergence of the distribution of displacements to a Gaussian one as t increases.

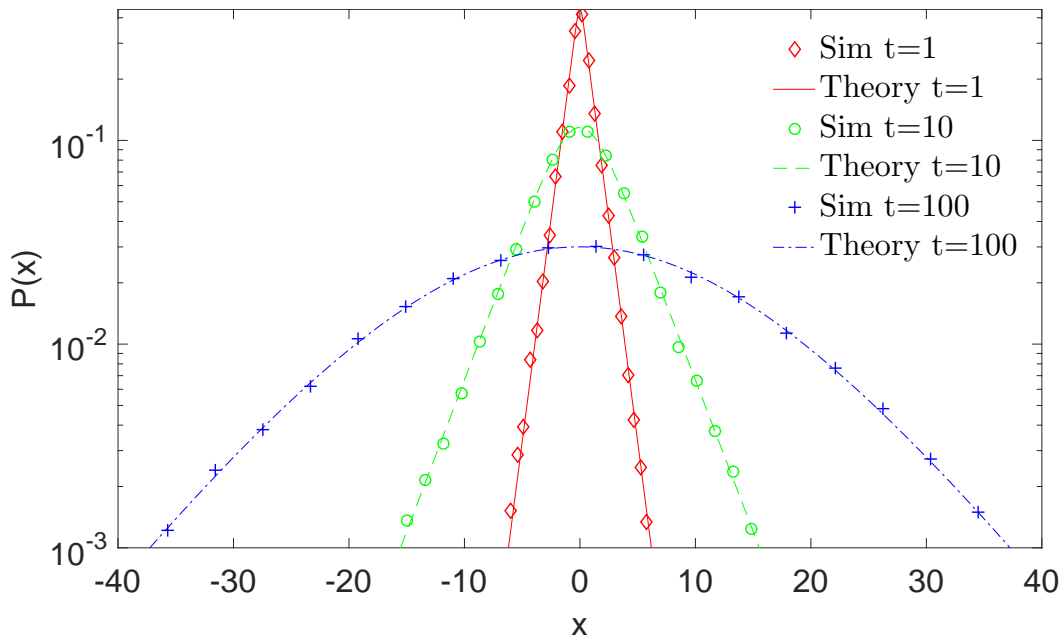


Figure 1. Distribution of displacements at times $t = \{1, 10, 100\}$. Here $\tau = 10$, $\bar{D} = 1$, $\sigma = 1/\sqrt{\tau}$ and thus $\nu = 1$. Theoretical results (lines) are compared to Monte Carlo simulations (symbols) with $M = 10^6$ particles.

Figure 2 shows the effect of the shape parameter ν on the distribution of displacements at time $t = 1$. The parameter ν changes the shape of the distribution. When $\nu \leq 1$, fluctuations are strong compared to both the average diffusivity \bar{D} and the correlation time τ . In this case, the probability of having strictly zero diffusivity is non zero $\mathbb{P}(D = 0) > 0$ [41]. Due to the accumulation at $D = 0$ the distribution of displacements becomes peaked near $x = 0$. In turn the distribution gets closer and closer to Gaussian as $\nu \rightarrow \infty$ (see Sec. 3.1).

On the length scale $\sigma\tau$, the diffusivity remains roughly the same. Intuitively, if $\sqrt{\bar{D}t} \ll \sigma\tau$, a particle has not enough time to explore the system. The distribution $P(x, t|x_0)$ could be considered as a superstatistical description of independent particles with constant but randomly chosen diffusion coefficients (see Sec. 3.2). Inversely, when

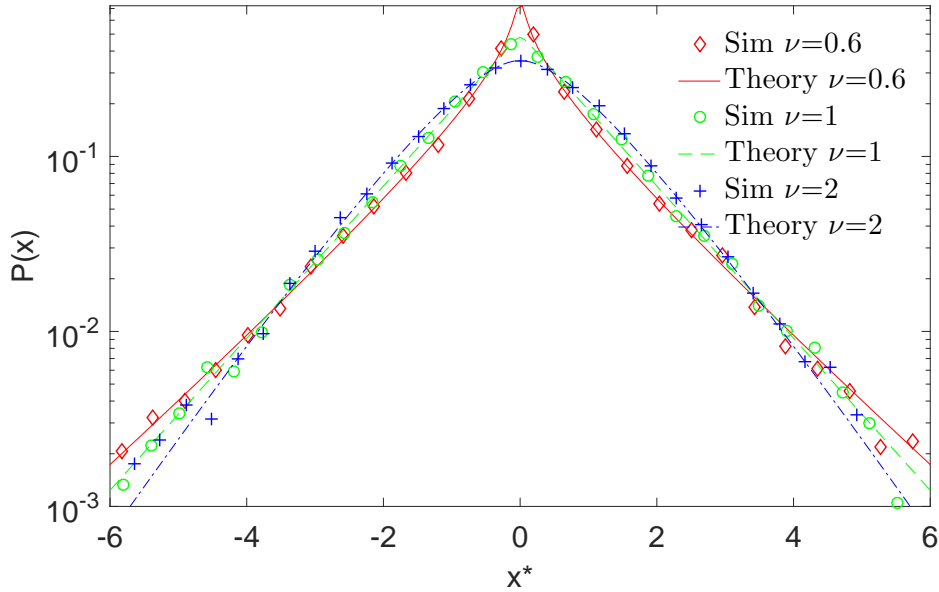


Figure 2. Distribution of normalized displacements, with $x^* = x/\sqrt{Dt}$, at fixed time $t = 1$ for different parameters $\nu = \{0.6, 1, 2\}$. For each case, we kept $\bar{D} = 1$ and $\tau = 100$ and varied σ . Theoretical results (lines) are compared to Monte Carlo simulations (symbols) with $M = 10^6$ particles.

$\sqrt{Dt} \gg \sigma\tau$, the particle has enough time to explore the medium and the distribution progressively becomes Gaussian. We introduce thus the time-dependent dimensionless diffusion length:

$$\mu(t) = \frac{\sqrt{Dt}}{\sigma\tau}. \quad (12)$$

As $\mu(t) \rightarrow \infty$, the particle explores the space beyond the correlation length, and the distribution gets closer to a Gaussian one. We show in Fig. 3 how $\mu(t)$ impacts the shape of the distribution. For instance at $\mu(t) = 1$, the distribution is almost Gaussian. When $\mu(t)$ decreases, the distribution becomes more peaked. The quantity $\mu(t)$ is directly related to the non-Gaussian parameter (see Eq. (27)).

Figure 4 illustrates trajectories and corresponding displacements. The envelop of time series of displacements shows patterns of fluctuations correlated on timescale τ . For small τ , the envelop becomes constant as in the Brownian motion case.

3. Asymptotic behavior

3.1. Brownian limit

We first consider the limiting case $\sigma\tau \rightarrow 0$, which can either be interpreted as diffusivity behaving deterministically ($\sigma \rightarrow 0$) or the mean reversion significantly stronger than fluctuation of diffusivity ($\tau \rightarrow 0$). In this limit one recovers $\tilde{P}(q, t) = e^{-q^2 Dt}$, from

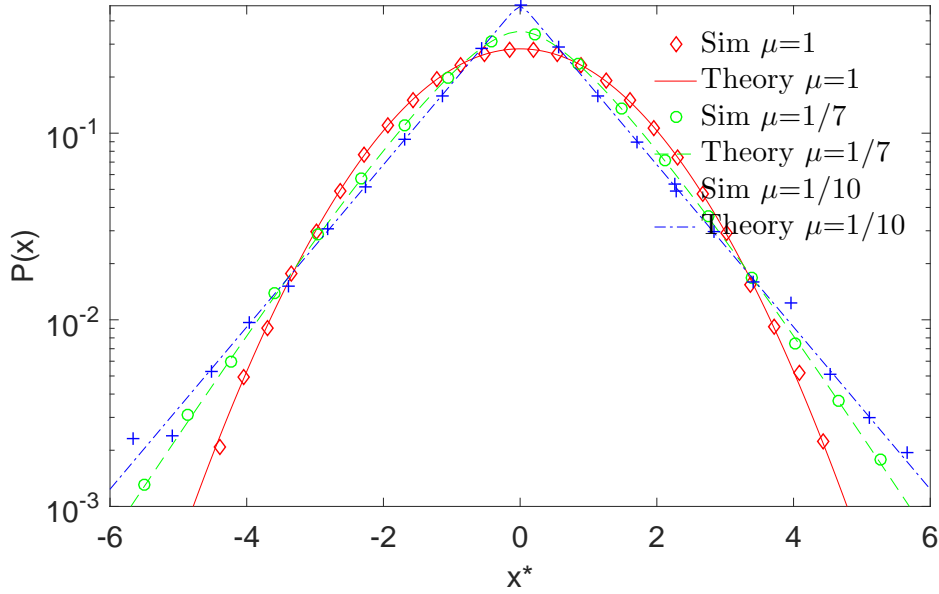


Figure 3. Distribution of normalized displacements, with $x^* = x/\sqrt{\bar{D}t}$, at fixed time $t = 1$, with $\mu(t)$ from Eq. (12) being varied in the range $\{1/10, 1/7, 1\}$ corresponding to $\nu = \{1, 2, 100\}$, by changing σ and keeping $\bar{D} = 1$ and $\tau = 100$. Theoretical results (lines) are compared to Monte Carlo simulations (symbols) with $M = 10^6$ particles.

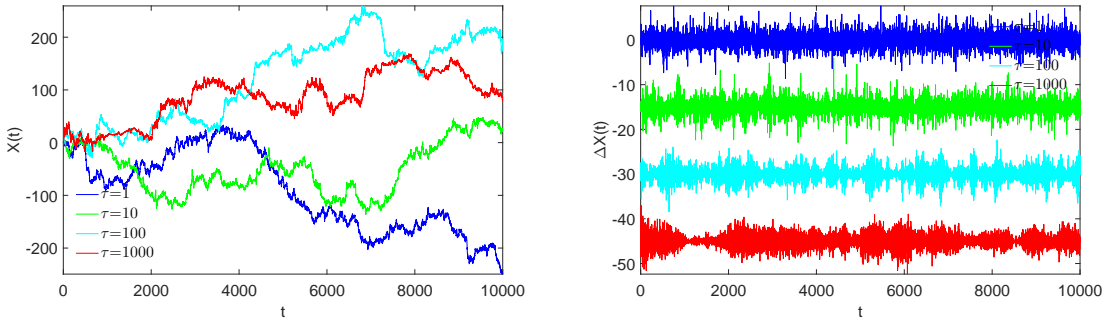


Figure 4. *Left.* Trajectories simulated for several values of $\tau = \{1, 10, 100, 1000\}$. Here ν is kept equal to one, with $\bar{D} = 1$ and $\sigma = 1/\sqrt{\tau}$. *Right.* Corresponding time series of position increments with lag-time $\delta t = 1$. For clarity, the time series are artificially shifted (with increasing τ values from top to bottom), but remain with zero mean.

which the Gaussian propagator for Brownian motion is retrieved:

$$P(x, t|x_0) = \frac{1}{\sqrt{4\pi\bar{D}t}} \exp\left(-\frac{(x-x_0)^2}{4\bar{D}t}\right). \quad (13)$$

This distribution also corresponds to the limit $\nu \rightarrow \infty$.

3.2. Short-time behavior

The superstatistical approach [34, 35] consists in writing the distribution of displacements as a superposition of Gaussian distributions weighted by a stationary distribution of diffusivity. In a recent work, Chechkin *et al.* [39] showed that non-Gaussian diffusion can be described at short times by superstatistics. Since during the correlation time τ , diffusivity does not evolve much, one can imagine an ensemble of particles with independent diffusivities. In our model, we use this relation to establish the short-time behavior.

One can relate our approach to the superstatistical approach in the following terms. At short times we have

$$x_t = \int_0^t \sqrt{2D_s} dW_s^{(1)} \approx \sqrt{2D_0} W_t^{(1)}, \quad (14)$$

and consider D_0 in the stationary regime. This short-time description loses track of the dynamics. We calculate $P_0(r, t)$, the probability to be at distance r from the starting point in d dimensions, where the subscript 0 highlights that it is a short-time description:

$$P_0(r, t) = \int_0^\infty dD_0 \Pi(D_0) \frac{1}{(4\pi D_0 t)^{d/2}} \exp\left(-\frac{r^2}{4D_0 t}\right), \quad (15)$$

with the stationary distribution $\Pi(D_0)$ of the CIR model from Eq. (7), which gives

$$P_0(r, t) = \frac{2^{1-\nu-d/2} \nu^{d/2}}{\Gamma(\nu) (\pi \bar{D} t)^{d/2}} \left(r \sqrt{\frac{\nu}{\bar{D} t}}\right)^{\nu-d/2} K_{\nu-d/2} \left(r \sqrt{\frac{\nu}{\bar{D} t}}\right), \quad (16)$$

where $K_\alpha(x)$ is the modified Bessel function of the second kind. Using the small x expansion of $K_\alpha(x)$, one gets for $\nu > d/2$

$$P_0(r=0, t) = \frac{\Gamma(\nu - d/2)}{\Gamma(\nu) (4\pi t)^{d/2}} \left(\frac{\nu}{\bar{D}}\right)^{d/2}. \quad (17)$$

In the case $\nu = 1$ and $d = 1$, the distribution is purely exponential

$$P_0(r, t) = \frac{1}{2\sqrt{\bar{D}t}} \exp\left(-\frac{r}{\sqrt{\bar{D}t}}\right) \quad (18)$$

(note that in this case the displacement r is distributed over $(-\infty, \infty)$). This approach is applicable at short times ($\mu(t) < 1$) but fails at long times because the underlying processes are fundamentally different. One can compare our model to this approach by calculating the non-Gaussian parameter

$$\gamma(t) = \frac{1}{3} \frac{\langle X^4(t) \rangle}{\langle X^2(t) \rangle^2} - 1, \quad (19)$$

which is equal to the excess kurtosis divided by 3 (the kurtosis of the Gaussian distribution). By definition, the non-Gaussian parameter is zero for the Gaussian distribution. For superstatistics with $d = 1$ and $x_0 = 0$, the MSD is $\langle x^2(t) \rangle_0 = 2\bar{D}t$ and the fourth moment $\langle x^4(t) \rangle_0 = 12t^2 \bar{D}^2 \frac{\nu+1}{\nu}$, which leads to the non-Gaussian parameter:

$$\gamma_0(t) = \frac{1}{\nu}. \quad (20)$$

In contrast to our model (see Sec. (4.1)), at all times the distribution of displacements spreads but does not change its shape: changing time just rescales space coordinates of the distribution. From this argument it is clear that the only way to reproduce convergence to a Gaussian distribution at long times is to make the stationary distribution $\Pi(D_0)$ of diffusivity time-dependent, which does not make sense. This is a branching point among non-Gaussian models, as constant or vanishing non-Gaussian parameter implies different microscopic mechanisms. Note that the distinction between interpretations can also be made using the autocorrelation of diffusivity: it is a delta function $\delta(\tau)$ in a superstatistical approach and an exponentially vanishing function in our model (see Sec. 4.2).

3.3. Large x behavior

We investigate the asymptotic behavior of the propagator at large $|x - x_0| \rightarrow \infty$. Here we only summarize the results, while the derivation is detailed in Appendix E. In the case $\nu = 1$, we obtain

$$P(x, t|x_0) \propto \exp\left(-\frac{|x - x_0|\beta_{t^*}}{2\sigma\tau}\right) \quad (|x - x_0| \rightarrow \infty), \quad (21)$$

with $\beta_{t^*} = \sqrt{1 + (4\alpha_{t^*}/t^*)^2}$, $t^* = t/\tau$ and α_{t^*} the smallest positive solution of

$$\alpha_{t^*} \sin \alpha_{t^*} = \frac{t^*}{4} \cos \alpha_{t^*}. \quad (22)$$

This agrees with experimental observations of a distribution of displacements with exponential tails [23, 24, 25]. When $\nu > 1$ is an integer, one gets power law corrections to the exponential decay:

$$P(x, t|x_0) \propto |x - x_0|^{\nu-1} \exp\left(-\frac{|x - x_0|\beta_{t^*}}{2\sigma\tau}\right) \quad (|x - x_0| \rightarrow \infty). \quad (23)$$

We expect that the same asymptotic behavior remains valid for any $\nu > 0$ (even non-integer), although its rigorous demonstration requires much finer analysis and is beyond the scope of this article. We conclude that the propagator exhibits a universal exponential decay at large increments, whereas the value of ν determines the power law corrections.

4. Statistical properties

In this section we describe the statistical properties of our model.

4.1. Moments and the non-Gaussian parameter

First we calculate the second and fourth moments using the relation

$$\langle X^k(t) \rangle = (-i)^k \frac{\partial^k}{\partial q^k} \tilde{P}(q, t)|_{q=0}, \quad (24)$$

where $\langle \cdot \rangle$ denotes the expectation. The second moment reads

$$\langle X^2(t) \rangle = 2\bar{D}t. \quad (25)$$

We observe thus the mean square displacement growing linearly with time, as in the Brownian case. In Sec. 5, an extension to anomalous diffusion through scaling arguments is proposed.

The process described in this article possesses many characteristics which are not deducible from the MSD. So we go further and calculate the fourth moment:

$$\langle X^4(t) \rangle = 12\bar{D}^2t^2 + 24\sigma^2\bar{D}\tau^2t + 24\sigma^2\bar{D}\tau^3(e^{-t/\tau} - 1). \quad (26)$$

From the second and fourth moments, we calculate the non-Gaussian parameter (see Eq. (19)). From Eqs.(25,26) the non-Gaussian parameter reads

$$\gamma(t) = \frac{2\sigma^2\tau^2}{\bar{D}t} \left(1 - \frac{1}{t/\tau} (1 - e^{-t/\tau}) \right). \quad (27)$$

As $t \rightarrow \infty$, the distribution slowly converges to a Gaussian distribution, as $1/t$. The theoretical formula is verified by simulations (Fig. 5). The leading term can be expressed in term of $\mu(t)$ as $\frac{2\sigma^2\tau^2}{\bar{D}t} = \frac{1}{2}\mu(t)^{-2}$ (see Eq. (12)), which shows that non-Gaussianity is related to space exploration, but the complete description also requires to take in account the correction terms from memory effects. Interestingly, we obtained the same form of $\gamma(t)$ as in the Kärger model [31, 32] with a finite number of equilibrium states (i.e. diffusivities), due to the averaging over diffusivity disorder (see also Sec. 5.1). The same results are evidently valid for the diffusivity modeled as the distance from the origin of an n -dimensional Ornstein-Uhlenbeck process [39, 37].

4.2. Autocorrelation of squared increments

Diffusing diffusivity models introduce a new level of complexity, far beyond the reach of the mean square displacement analysis, and new tools are needed to describe such processes. A wide range of models with fluctuating volatility (or diffusivity in physical language) have already been studied in finance [41, 42, 43]. Since the square of an increment is a local measure of diffusivity, its autocorrelations can reveal information on memory effects of diffusivity. On one hand, it is possible to evaluate the autocorrelation of diffusivity directly from a given trajectory by calculating the autocorrelation of its squared increments. On the other hand, this quantity is accessible theoretically.

Let us define the centered squared increment $dx_t^{2*} = dx_t^2 - \langle dx_t^2 \rangle$. Generally, one gets (see Appendix D for details)

$$\langle dx_t^{2*} dx_{t+\Delta}^{2*} \rangle = \begin{cases} 12\langle D_t^2 \rangle - 4\langle D_t \rangle^2 & (\Delta = 0), \\ 4\langle D_t D_{t+\Delta} \rangle - 4\langle D_t \rangle \langle D_{t+\Delta} \rangle & (\Delta > 0). \end{cases} \quad (28)$$

In our model, we find

$$\langle dx_t^{2*} dx_{t+\Delta}^{2*} \rangle = \begin{cases} 12\sigma^2\tau(1 - e^{-t/\tau})^2 \left[\bar{D} + 2D_0 \frac{e^{-t/\tau}}{1 - e^{-t/\tau}} \right] + \\ \quad 8((D_0 - \bar{D})e^{-t/\tau} + \bar{D})^2 & (\Delta = 0), \\ 4e^{-\Delta/\tau} \left[\sigma^2\bar{D}\tau(1 - e^{-t/\tau})^2 + 2\sigma^2\tau D_0(e^{-t/\tau} - e^{-2t/\tau}) \right] & (\Delta > 0). \end{cases} \quad (29)$$

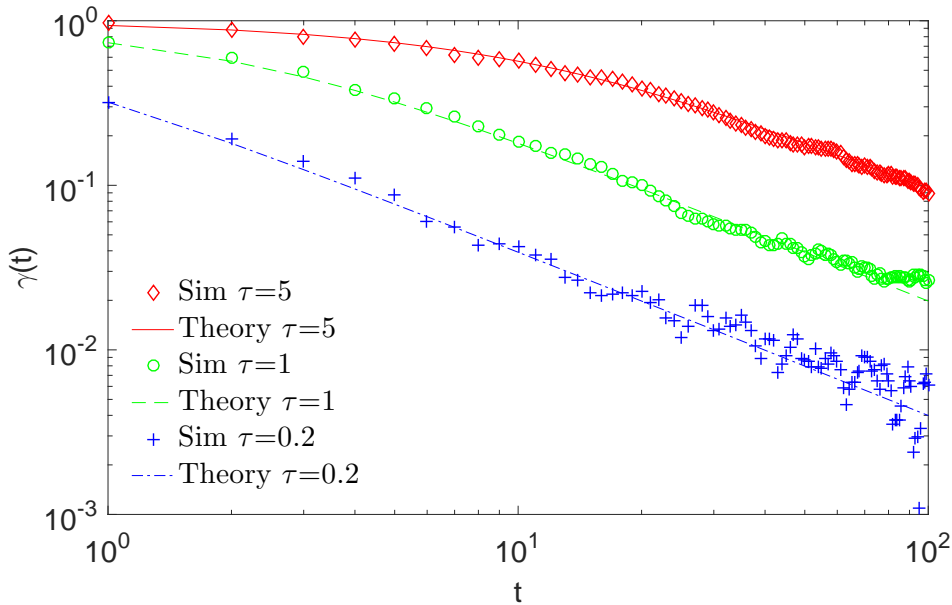


Figure 5. The non-Gaussian parameter calculated from Eq. (27) (lines) and from Monte Carlo simulations (symbols) with $M = 10^5$ particles, for different values of $\tau = \{0.2, 1, 5\}$, while keeping $\nu = 1$, $\bar{D} = 1$ and $\sigma = 1/\sqrt{\tau}$.

One notes the exponentially vanishing dependence on initial conditions. In the long-time limit $t \rightarrow \infty$, one simply gets

$$\lim_{t \rightarrow \infty} \langle dx_t^{2*} dx_{t+\Delta}^{2*} \rangle = \begin{cases} 12\sigma^2 \bar{D} \tau + 8\bar{D}^2 & (\Delta = 0), \\ 4\sigma^2 \bar{D} \tau e^{-\Delta/\tau} & (\Delta > 0). \end{cases} \quad (30)$$

The mean-reverting property of the CIR model results in the exponential autocorrelation of diffusivity. If an experimentally measured autocorrelation of squared increments is not exponentially vanishing, the mean reverting property cannot be described by a simple harmonic potential centered on \bar{D} , and thus another model (or an extension of the present model) should be considered.

4.3. Ergodicity and finite sample effects

Data analysis is usually performed with time-averaged quantities because of small data samples. Then a natural question of equivalence between time and ensemble averages arises: “Is a time-averaged quantity from one particle representative of other particles from the same system?”. For a system at thermodynamical equilibrium, the time average over an infinitely long trajectory matches the ensemble average over an infinite number of particles, this statement is known as the ergodicity hypothesis.

From the Langevin equation (2), one can directly see that our model is ergodic: as the diffusivity is fluctuating around its average, fluctuations will be averaged out in the limit of infinitely long trajectories. But for a finite duration of experiment, what can be said about ergodicity of the system?

If the experiment duration t_{exp} is shorter than the time to explore heterogeneities of the system, $t_{exp} < t_{sys}$, different tracers probe regions with different diffusivities. As a consequence, on such a timescale, tracers would appear as experiencing different dynamics, so that one could wrongly conclude that the dynamics of the system is nonergodic. Inversely, if the experiment is sufficiently long (i.e. $t_{exp} \gg t_{sys}$), tracers have enough time to visit every region of the system, and one concludes correctly that the ergodicity hypothesis is fulfilled. As a consequence, the experiment duration plays an important role and should be chosen accurately.

To illustrate this point we study two quantities characterizing ergodicity by different strategies. We show that depending on the parameters of the model, the results of the tests can sound contradictory. First we use the Ergodicity Breaking parameter $EB(\Delta, t_{exp})$ [44, 45, 46] which quantifies the dispersion of the time-averaged MSD $\bar{\delta}^2(\Delta, t_{exp})$ [47, 12, 48] with

$$\bar{\delta}^2(\Delta, t_{exp}) = \frac{1}{t_{exp} - \Delta} \sum_{n=1}^{t_{exp}-\Delta} (x_{n+\Delta} - x_n)^2 \quad (31)$$

as a function of the experiment duration t_{exp} (i.e. the trajectory length) evaluated with a time-lag Δ :

$$EB(\Delta, t_{exp}) = \frac{\langle (\bar{\delta}^2(\Delta, t_{exp}))^2 \rangle}{\langle \bar{\delta}^2(\Delta, t_{exp}) \rangle^2} - 1. \quad (32)$$

For an ergodic process, $\lim_{t_{exp} \rightarrow \infty} EB(\Delta, t_{exp}) = 0$ for any Δ , meaning that for a fixed Δ , the distribution of TAMSD converges to a Dirac delta function with $\bar{\delta}^2(\Delta, t_{exp} \rightarrow \infty) = \langle X^2(\Delta) \rangle$.

Figure 6 shows that fluctuations of TAMSD are impacted by two characteristics: the shape parameter ν and the correlation time τ . The smaller the parameter ν , the longer it takes for the EB parameter to vanish. Indeed, for $\nu \leq 1$, diffusivity can be 0 with positive probability that would slow down the dynamics. The correlation time τ also influences the convergence of $EB(\Delta, t_{exp})$: larger τ implies longer time to recover from small diffusivities and thus slower dynamics. Setting $\nu = 1$ and varying τ , the EB parameter has a transient behavior until $\approx 2\tau$ and decays as a power law $1/t_{exp}$ as in the Brownian case for which the exact formula is $EB(\Delta, t_{exp}) = \frac{(2\Delta+1/\Delta)}{3(t_{exp}-\Delta+1)}$ [49]. Note that a slow decrease of the EB parameter due to disorder was also discussed for fluctuating diffusivity [50] and diffusion in a periodic potential [51].

We also present the result from the ergodicity test based on the dynamical functional [52, 53]. An ergodic process has a vanishing velocity autocorrelation function so two fragments of the trajectory become independent when time between them is sufficiently long. The ergodicity estimator $\tilde{F}_\omega(\Delta, t_{exp})$ measures how long it takes before independence is verified on the characteristic function. It has been shown [52] that for any stationary infinitely divisible ergodic process this function asymptotically vanishes, as also verified by calculating the mean estimator $\langle \tilde{F}_\omega(\Delta, t_{exp}) \rangle$ [53] in the case of fractional Brownian motion. In contrast, the mean estimator never vanishes in the

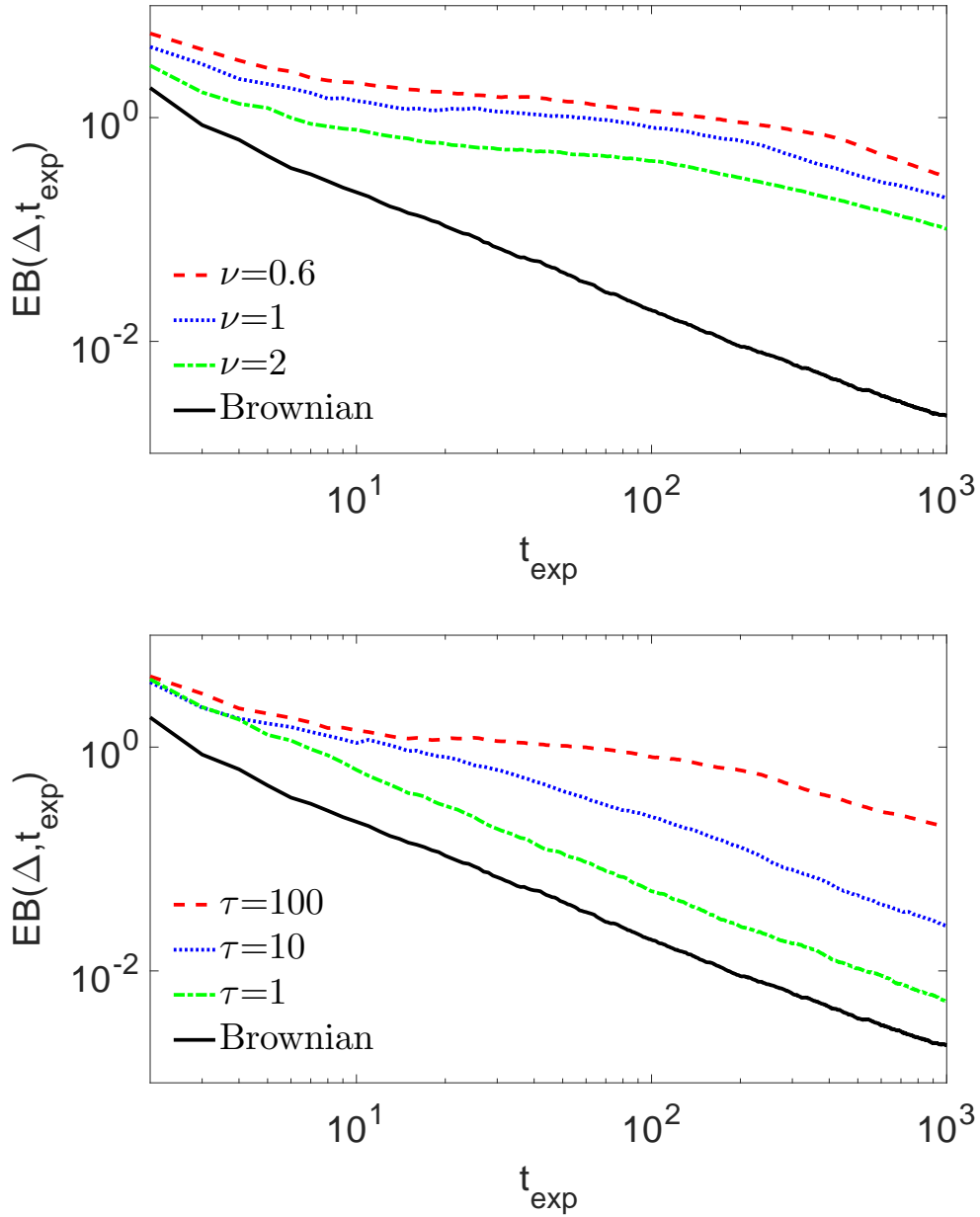


Figure 6. Ergodicity breaking parameter calculated by averaging over $M = 10^3$ simulated trajectory of length $t_{exp} = 10^3$. The result for Brownian motion (solid line) is also plotted for comparison. *Top.* Results for variable shape parameter $\nu = \{0.6, 1, 2\}$ by varying τ , with $\bar{D} = 1$ and $\sigma = 1$ being constant. *Bottom.* Results for variable correlation time $\tau = \{1, 10, 100\}$ while keeping $\nu = 1$, $\bar{D} = 1$ and $\sigma = 1/\sqrt{\tau}$.

case of nonergodic continuous time random walk. In Fig. 7, the estimator $\tilde{F}_\omega(\Delta, t_{exp})$ decays fast so that the temporal disorder due to diffusivity does not affect much this quantity, in contrast to the EB parameter.

If this estimator vanishes for a single particle trajectory, one can expect asymptotic independence and ergodicity. This implies that getting longer data indeed increases the

accuracy of time averaged quantities (smaller $EB(\Delta, t_{exp})$).

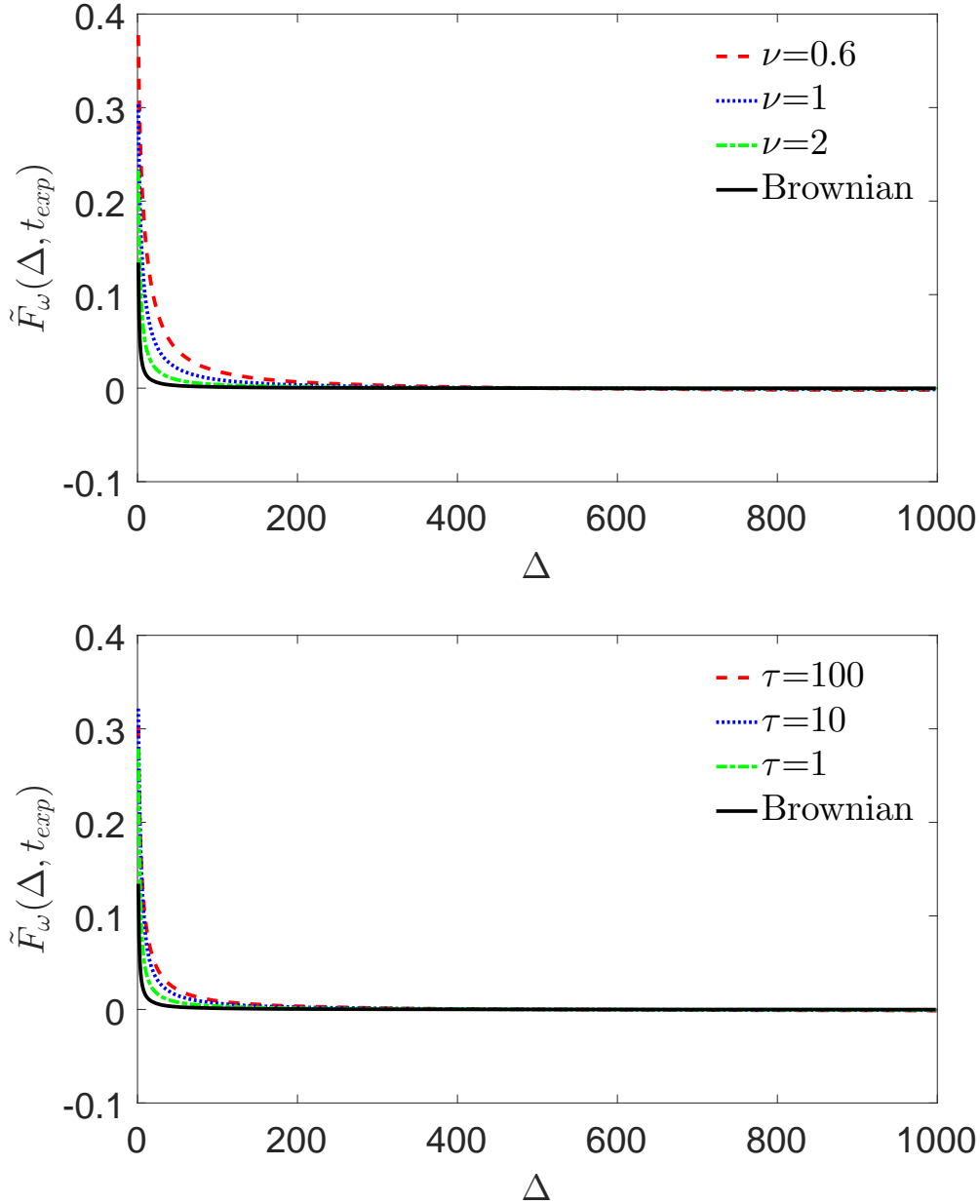


Figure 7. Mean ergodicity estimator $\tilde{F}_\omega(\Delta, t_{exp})$, calculated with $M = 10^3$ simulated trajectories of length $t_{exp} = 10^3$. The mean estimator for Brownian motion (solid line) is also plotted for comparison. *Top.* Different values of the shape parameter $\nu = \{0.6, 1, 2\}$ by varying τ , with $\bar{D} = 1$ and $\sigma = 1/\sqrt{\tau}$. *Bottom.* Different values of $\tau = \{1, 10, 100\}$ while keeping $\nu = 1$, $\bar{D} = 1$ and $\sigma = 1/\sqrt{\tau}$.

The ergodicity breaking parameter shows that the distribution of TAMSD slowly converges to a delta function. In turn, the ergodicity estimator $\tilde{F}_\omega(\Delta, t_{exp})$ indicates that the process loses its memory and implies that the TAMSD distribution narrows with increasing t_{exp} (without specifying how). These two quantities do not answer the

ergodicity question in the same way, they are complementary. If one needs to know the degree of dispersion of TAMSD, the EB parameter has to be used. The estimator $\tilde{F}_\omega(\Delta, t_{exp})$, which can be applied to a single trajectory, does not quantifies fluctuations, but allows to verify ergodicity, even in the presence of dynamic disorder because it relies on the estimation of the characteristic function of the process.

5. Discussion

5.1. Fourth moment is not sufficient

The Kärger model [31] has been developed to study diffusion in a medium in which a particle can randomly switch between two domains with distinct diffusion coefficients D_1 and D_2 , with the exchange rates K_{12} and K_{21} . By solving two coupled diffusion-reaction equations, the Fourier transform of the propagator can be derived [31]

$$\tilde{F}_{KM}(q, t) = (1 - p') \exp(-q^2 D'_1(q)t) + p' \exp(-q^2 D'_2(q)t), \quad (33)$$

with

$$\begin{aligned} D'_1(q) &= \frac{1}{2} \left(D_1 + D_2 + \frac{1}{q^2} (K_{12} + K_{21}) \right. \\ &\quad \left. - \left(\left(D_2 - D_1 + \frac{1}{q^2} (K_{21} - K_{12}) \right)^2 + \frac{4K_{12}K_{21}}{q^4} \right)^{1/2} \right), \\ D'_2(q) &= \frac{1}{2} \left(D_1 + D_2 + \frac{1}{q^2} (K_{12} + K_{21}) \right. \\ &\quad \left. + \left(\left(D_2 - D_1 + \frac{1}{q^2} (K_{21} - K_{12}) \right)^2 + \frac{4K_{12}K_{21}}{q^4} \right)^{1/2} \right), \\ p' &= \frac{1}{D'_2(q) - D'_1(q)} (p_1 D_1 + p_2 D_2 - D'_1(q)), \end{aligned} \quad (34)$$

where p_1 and p_2 are relative volume fractions of two domains. The analytical expression of the non-Gaussian parameter, which was derived in [54], and also studied in [32], has the same functional form as $\gamma(t)$ from Eq. (27):

$$\gamma_{KM}(t) = M_{KM,0} \frac{2}{t/\tau} \left(1 - \frac{1}{t/\tau} (1 - e^{-t/\tau}) \right), \quad (35)$$

with the coefficient $M_{KM,0} = \frac{p_1 p_2 (D_1 - D_2)^2}{(p_1 D_1 + p_2 D_2)^2}$, which corresponds in our case to $\frac{\sigma^2 \tau}{D}$, and τ is the exchange time: $\tau = 1/K_{12} = 1/K_{21}$.

Figure 8 compares distributions for the Kärger model and our approach. The Kärger model as a superposition of only two Gaussian distributions does not match perfectly our model with infinitely many Gaussian distributions superimposed (see Sec. 3.2). In the case $\nu > 1$, both distributions are very close at all times. In the case $\nu \leq 1$, obtained here by setting different relative volumes p_1 and p_2 , the Kärger model does not reproduce the peak at 0.

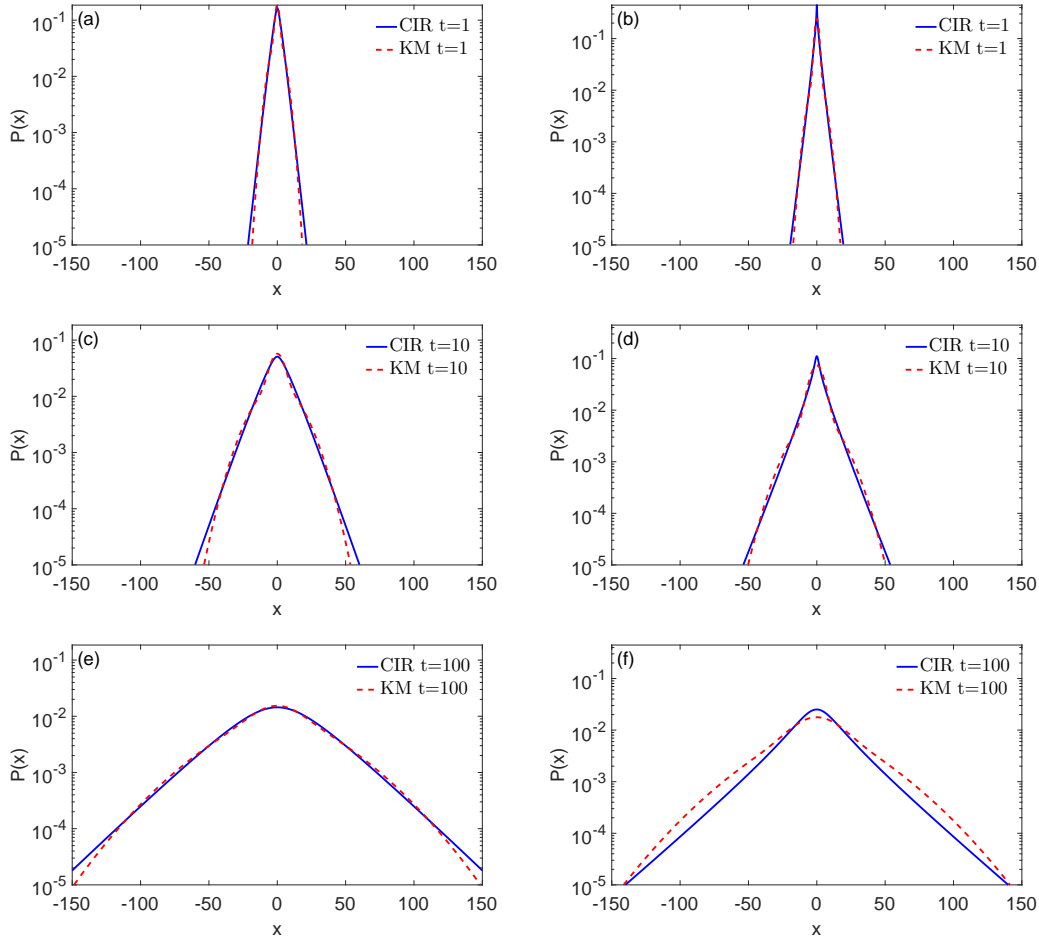


Figure 8. Distribution of displacements for the Kärger model (dashed lines) and our model (solid lines) at time $t = 1$ (top), $t = 10$ (middle), $t = 100$ (bottom). We choose the parameters for the Kärger model and deduce $\bar{D} = p_1 D_1 + p_2 D_2$ and $\sigma = \sqrt{\bar{D} M_{KM,0}/\tau}$. *Left column.* Parameters of the Kärger model are $p_1 = 1/2$, $p_2 = 1/2$, $D_1 = 1$ and $D_2 = 10$ and $\tau = 10$, leading to $\nu \approx 1.5$. *Right column.* Parameters of the Kärger model are $p_1 = 4/5$, $p_2 = 1/5$, $D_1 = 1$ and $D_2 = 10$ and $\tau = 10$, leading to $\nu \approx 0.6$.

We conclude that these two distributions can have identical second and fourth moments, but are still different. While it was known that mean squared displacement is not sufficient to characterize a model, here we illustrate that even the fourth moment (and the non-Gaussian parameter) is not enough.

5.2. Anomalous diffusion

In biology there are many experimental evidences of anomalous diffusion [1, 2, 3, 4, 5] when the mean squared displacement scales as a power law with time $\langle X^2(t) \rangle = 2D_\alpha t^\alpha$ where D_α is the generalized diffusion coefficient and α is the anomalous exponent. We propose an extension by a simple scaling of the time $t/\tau \Rightarrow (t/\tau)^\alpha$, so that $\tilde{P}(q, t)$ from

Eq. (9) is replaced by

$$\tilde{P}(q, t) = \left(e^{-\frac{1}{2}(\omega-1)(t/\tau)^\alpha} \frac{4\omega}{(\omega+1)^2} \left(1 - \left(\frac{\omega-1}{\omega+1} \right)^2 e^{-\omega(t/\tau)^\alpha} \right)^{-1} \right)^\nu. \quad (36)$$

The non-Gaussian parameter would now depend on α :

$$\gamma(t) = \frac{2\sigma^2\tau^{1+\alpha}}{\bar{D}t^\alpha} \left(1 - \frac{1}{(t/\tau)^\alpha} (1 - e^{-(t/\tau)^\alpha}) \right). \quad (37)$$

As expected, in the subdiffusive case $\alpha < 1$, the convergence to a Gaussian distribution is slower as compared to the superdiffusive case $\alpha > 1$, because larger α means faster exploration of space.

6. Conclusion

We presented a model of non-Gaussian diffusion, based on coupled Langevin equations. We derived the explicit exact formula for the distribution of displacements in the Fourier domain and studied different asymptotic regimes. We showed that this distribution exhibits exponential tails and converges slowly, as $1/t$, to a Gaussian one. The MSD evolves linearly with time in spite of non-Brownian character of the motion. We pointed that the ergodicity estimator $\tilde{F}_\omega(\Delta, t_{exp})$ catches ergodic nature of the process while the random nature of diffusivity makes fluctuations of TAMSD to span up at long times as demonstrated by the ergodicity breaking parameter $EB(\Delta, t_{exp})$. We used the autocorrelation of squared increments to determine the autocovariance structure of diffusivity. We expect that this model will help to understand more deeply dynamical heterogeneities observed in experiments. An important perspective is to relate the correlation structure of the stochastic diffusivity D_t to eventual models of space-dependent diffusivity $D(x_t)$.

Acknowledgments

DG acknowledges the financial support by French National Research Agency (ANR Project ANR-13-JSV5-0006-01). The authors thank Dr. Aleksei Chechkin, Dr. Dimitri Novikov and Dr. Marcel Filoche for inspiring discussions.

Appendix A. Derivation of the Cox-Ingersoll-Ross equation

Consider a collection of independent Ornstein-Uhlenbeck processes indexed by $i \in [1, n]$, each of them obeying the Langevin equation:

$$dY_t^{(i)} = -\frac{1}{2}\beta Y_t^{(i)} dt + \frac{\sqrt{2}}{2}\sigma dW_t^{(i)}, \quad (A.1)$$

where β is the inverse correlation time, σ is the level of fluctuations, and $W_t^{(i)}$ are independent Wiener processes. Following [36, 39] the diffusing diffusivity is modeled as

$$D_t = \sum_{i=1}^n \left(Y_t^{(i)} \right)^2. \quad (\text{A.2})$$

Let $f(y_1, y_2, \dots, y_n) = \sum_{i=1}^n y_i^2$ so that $\frac{\partial}{\partial y_i} f = 2y_i$ and $\frac{\partial^2}{\partial y_i \partial y_j} f = 2\delta_{ij}$.

According to Itô formula, we get

$$\begin{aligned} dD_t &= \sum_{i=1}^n \frac{\partial}{\partial y_i} f dY_t^{(i)} + \frac{1}{2} \sum_{i,j=1}^n \frac{\partial^2}{\partial y_i \partial y_j} f dY_t^{(i)} dY_t^{(j)} \\ &= \sum_{i=1}^n 2Y_t^{(i)} \left(-\frac{1}{2}\beta Y_t^{(i)} dt + \frac{\sqrt{2}}{2}\sigma dW_t^{(i)} \right) + \sum_{i=1}^n \left(-\frac{1}{2}\beta Y_t^{(i)} dt + \frac{\sqrt{2}}{2}\sigma dW_t^{(i)} \right)^2 \\ &= \sum_{i=1}^n 2Y_t^{(i)} \left(-\frac{1}{2}\beta Y_t^{(i)} dt + \frac{\sqrt{2}}{2}\sigma dW_t^{(i)} \right) + \frac{1}{2}n\sigma^2 dt \\ &= \left(\frac{1}{2}n\sigma^2 - \beta \sum_{i=1}^n \left(Y_t^{(i)} \right)^2 \right) dt + \sum_{i=1}^n \sigma \sqrt{2} Y_t^{(i)} dW_t^{(i)} \\ &= \left(\frac{1}{2}n\sigma^2 - \beta D_t \right) dt + \sqrt{2}\sigma \sum_{i=1}^n Y_t^{(i)} dW_t^{(i)} \\ &= \left(\frac{1}{2}n\sigma^2 - \beta D_t \right) dt + \sigma \sqrt{2D_t} \sum_{i=1}^n \frac{Y_t^{(i)}}{\sqrt{D_t}} dW_t^{(i)}. \end{aligned}$$

The stochastic process W_t defined as $W_t = \sum_{i=1}^n \int_0^t \frac{Y_s^{(i)}}{\sqrt{D_s}} dW_s^{(i)}$ is a martingale because it has no drift [55]. For its increments, $dW_t = \sum_{i=1}^n \frac{Y_t^{(i)}}{\sqrt{D_t}} dW_t^{(i)}$, we verify that

$dW_t dW_t = \sum_{i=1}^n \frac{(Y_t^{(i)})^2}{D_t} \left(dW_t^{(i)} \right)^2 = dt$, so the increments are properly normalized. We conclude that W_t is a Wiener process.

We now can rewrite the above equation as:

$$dD_t = \left(\frac{1}{2}n\sigma^2 - \beta D_t \right) dt + \sigma \sqrt{2D_t} dW_t. \quad (\text{A.3})$$

Setting $\beta = 1/\tau$ and $n = 2\frac{\bar{D}}{\sigma^2\tau} = 2\nu$ one finally retrieves the Cox-Ingersoll-Ross equation

$$dD_t = \frac{1}{\tau} (\bar{D} - D_t) dt + \sigma \sqrt{2D_t} dW_t. \quad (\text{A.4})$$

Appendix B. Solution of the equation

The method of solution is inspired from [25] where the probability distribution of returns of the Heston model was derived. We consider the two-dimensional forward Fokker-Planck equation (3) on position and diffusivity with the initial condition $P(x, D, t =$

$$0|x_0, D_0) = \delta(x - x_0)\delta(D - D_0).$$

This equation can be solved by transforming the position x into the Fourier space, and the diffusivity, defined on the real half line $D \in [0, \infty)$, into the Laplace space:

$$\tilde{P}(q, s, t|x_0, D_0) = \int_{-\infty}^{\infty} dx \int_0^{\infty} dD e^{-iqx - Ds} P(x, D, t|x_0, D_0). \quad (\text{B.1})$$

This leads to the first-order partial differential equation:

$$\frac{\partial}{\partial t} \tilde{P} + G(s) \frac{\partial}{\partial s} \tilde{P} = -\frac{\bar{D}}{\tau} s \tilde{P}, \quad (\text{B.2})$$

with $G(s) = \sigma^2 (s - s_1)(s - s_2)$, where $s_1 = \frac{-\frac{1}{\tau} + \Omega}{2\sigma^2}$, $s_2 = \frac{-\frac{1}{\tau} - \Omega}{2\sigma^2}$, and $\Omega = \sqrt{\frac{1}{\tau^2} + 4\sigma^2 q^2}$. The initial condition is now $\tilde{P}(q, s, t = 0|x_0, D_0) = e^{-iqx_0} e^{-sD_0}$. We search for the solution in the following form:

$$\tilde{P}(q, s, t|x_0, D_0) = f(t - g(s)) h(s), \quad (\text{B.3})$$

with three unknown functions f, g, h . Nontrivial solutions are found by solving

$$\begin{cases} 1 - g'G = 0, \\ Gh' + \frac{\bar{D}}{\tau} sh = 0, \end{cases} \quad (\text{B.4})$$

which gives

$$\begin{cases} g(s) = \frac{1}{\Omega} \ln \left(\frac{s-s_1}{s-s_2} \right), \\ h(s) = (s-s_1)^{\frac{-\bar{D}}{\Omega\tau} s_1} (s-s_2)^{\frac{\bar{D}}{\Omega\tau} s_2}. \end{cases} \quad (\text{B.5})$$

Now we use the initial condition to deduce the function f :

$$\tilde{P}(q, s, t = 0|x_0, D_0) = e^{-iqx_0} e^{-sD_0} = f(-g(s)) h(s), \quad (\text{B.6})$$

from which we get

$$f(z) = \frac{e^{-iqx_0} e^{-D_0 g^{-1}(-z)}}{h(g^{-1}(-z))}, \quad (\text{B.7})$$

or equivalently,

$$f(z) = \left(\frac{\Omega}{\sigma^2} \right)^\nu e^{-iqx_0} \exp \left(-D_0 \frac{s_1 - s_2 e^{-\Omega z}}{1 - e^{-\Omega z}} \right) (1 - e^{-\Omega z})^{-\nu} e^{-\frac{\bar{D}s_1}{\tau} z}. \quad (\text{B.8})$$

The solution is finally

$$\begin{aligned} \tilde{P}(q, s, t|x_0, D_0) &= F(x_0, D_0, s) \left(\frac{\Omega}{\sigma^2} \right)^\nu (s - s_2 - (s - s_1)e^{-\Omega t})^{-\nu} \\ &\quad \times \exp \left(-\bar{D}/\tau \left(\frac{-\frac{1}{\tau} + \Omega}{2\sigma^2} \right) t \right), \end{aligned} \quad (\text{B.9})$$

with ν from Eq. (1) and

$$F(x_0, D_0, s) = \exp \left(-iqx_0 - D_0 \frac{s_1 - s_2 \frac{s-s_1}{s-s_2} e^{-\Omega t}}{1 - \frac{s-s_1}{s-s_2} e^{-\Omega t}} \right). \quad (\text{B.10})$$

Substituting s_1 and s_2 in Eq. (B.9) and Eq. (B.10), we get Eq. (6).

In practice, it is hard to access directly the time-dependent diffusivity. It is therefore convenient to integrate the joint probability over diffusivity to get the marginal distribution $\tilde{P}(q, t|x_0, D_0)$, which can be obtained in the Laplace domain by simply setting $s = 0$:

$$\begin{aligned} \tilde{P}(q, t|x_0, D_0) &= F(x_0, D_0, s=0|x_0) \left(\frac{\left(\frac{2\Omega}{\frac{1}{\tau} + \Omega}\right)}{1 - \left(1 - \frac{2\Omega}{\frac{1}{\tau} + \Omega}\right) e^{-\Omega t}} \right)^\nu \\ &\times \exp\left(-\bar{D}/\tau \left(\frac{-\frac{1}{\tau} + \Omega}{2\sigma^2}\right) t\right). \end{aligned} \quad (\text{B.11})$$

Another issue is the dependence on the initial diffusivity D_0 . If the system is in a stationary regime for the diffusivity, one can average over the stationary distribution $\Pi(D_0)$. This distribution can be obtained from Eq. (6) by averaging over position ($q = 0$), then taking the limit $t \rightarrow \infty$ and using the inverse Laplace transform relation

$$\Pi(D_0) = \mathcal{L}^{-1} \left[\left(s + \frac{1}{\sigma^2\tau} \right)^{-\nu} \right] = \frac{\nu^\nu}{\Gamma(\nu)\bar{D}^\nu} D_0^{\nu-1} \exp\left(-\frac{D_0}{\sigma^2\tau}\right), \quad (\text{B.12})$$

also known from [56]. Then, the average over initial diffusivity yields

$$\tilde{P}(q, t|x_0) = \int_0^\infty \Pi(D_0) \tilde{P}(q, t|x_0, D_0) dD_0. \quad (\text{B.13})$$

Taking the integral, we deduce Eq. (9).

Appendix C. Subordination

Subordination is an elegant mathematical tool to describe complex processes, in particular anomalous diffusion [57, 58]. Chechkin *et al.* [39] applied it in the diffusing diffusivity context by observing that the Fokker-Planck equation

$$\frac{\partial}{\partial t} P(x, t) = D(t) \frac{\partial^2}{\partial x^2} P(x, t), \quad (\text{C.1})$$

can be written in the subordinated form:

$$\begin{cases} \frac{\partial p(x, u)}{\partial u} = \frac{\partial^2}{\partial x^2} p(x, u), \\ \frac{\partial u}{\partial t} = D(t), \end{cases} \quad (\text{C.2})$$

where $p(x, u) = \frac{1}{\sqrt{4\pi u}} \exp\left(-\frac{x^2}{4u}\right)$ is the Gaussian propagator. Let $T(u, t)$ be the probability density of $u(t) = \int_0^t D(s) ds$. The solution of Eq. (C.1) can be expressed as

$$P(x, t) = \int_0^\infty p(x, u) T(u, t) du = \int_0^\infty \frac{e^{-\frac{x^2}{4u}}}{\sqrt{4\pi u}} T(u, t) du. \quad (\text{C.3})$$

Now the Fourier transform with respect to x yields:

$$\tilde{P}(q, t) = \int_0^\infty T(u, t) e^{-q^2 u} du = \tilde{T}(q^2, t), \quad (\text{C.4})$$

where $\tilde{T}(q^2, t)$ denotes the Laplace transform of T with respect to $s = q^2$. In our model, the description of diffusivity is made in term of the Cox-Ingersoll-Ross equation which reads

$$\frac{\partial \Pi(D, t | D_0)}{\partial t} = \frac{1}{\tau} \frac{\partial}{\partial D} [(D - \bar{D})\Pi] + \sigma^2 \frac{\partial^2}{\partial D^2} (D\Pi). \quad (\text{C.5})$$

In the Laplace domain, one has

$$\frac{\partial}{\partial t} \tilde{\Pi}(s, t) + G(s) \frac{\partial}{\partial s} \tilde{\Pi}(s, t) = -\frac{1}{\tau} \bar{D} s \tilde{\Pi}(s, t), \quad (\text{C.6})$$

with $G(s) = s(\sigma^2 s + \frac{1}{\tau})$. The initial condition is now $\tilde{\Pi}(s, t = 0 | D_0) = e^{-s D_0}$. The integral $\tilde{T}(s, t) = \int_0^t \tilde{\Pi}(s, t') dt'$ is known from [59]

$$\begin{aligned} T(s, t | D_0) &= \left[\frac{e^{t^*/2}}{\cosh(\omega_s t^*/2) + \frac{1}{\omega_s} \sinh(\omega_s t^*/2)} \right]^\nu \\ &\times \exp \left[-\frac{s D_0 \tau}{\omega_s} \frac{2 \sinh(\omega_s t^*/2)}{\cosh(\omega_s t^*/2) + \frac{1}{\omega_s} \sinh(\omega_s t^*/2)} \right], \end{aligned} \quad (\text{C.7})$$

with $t^* = t/\tau$ and $\omega_s = \sqrt{1 + 4s\sigma^2\tau^2}$. According to Eq. (C.4), one deduces thus the characteristic function as a function of initial diffusivity D_0 :

$$\begin{aligned} \tilde{P}(q, t | D_0) &= \left[\frac{e^{t^*/2}}{\cosh(\omega t^*/2) + \frac{1}{\omega} \sinh(\omega t^*/2)} \right]^\nu \\ &\times \exp \left[-\frac{D_0 q^2 \tau}{\omega} \frac{2 \sinh(\omega t^*/2)}{\cosh(\omega t^*/2) + \frac{1}{\omega} \sinh(\omega t^*/2)} \right], \end{aligned} \quad (\text{C.8})$$

with $\omega = \sqrt{1 + 4q^2\sigma^2\tau^2}$. After integration over initial diffusivity the characteristic function yields

$$\begin{aligned} \tilde{P}(q, t) &= \left[\frac{e^{t^*/2}}{\cosh(\omega t^*/2) + \frac{1}{\omega} \sinh(\omega t^*/2)} \right]^\nu \\ &\times \left(1 + \frac{2\sigma^2 q^2 \tau^2 \sinh(\omega t^*/2)}{\omega \cosh(\omega t^*/2) + (1 - 2\omega\sigma^2 q^2 \tau^2) \sinh(\omega t^*/2)} \right)^\nu. \end{aligned} \quad (\text{C.9})$$

This is an alternative representation of the characteristic function $\tilde{P}(q, t)$ from Eq. (8).

Appendix D. Autocorrelation of squared increments

We have $dx_t = \sqrt{2\bar{D}_t} dW_t^{(1)}$ and the diffusivity in the integral form reads

$$D_t = D_0 e^{-t/\tau} + \bar{D}(1 - e^{-t/\tau}) + e^{-t/\tau} \int_0^t e^{s/\tau} \sqrt{D_s} dW_s^{(2)}. \quad (\text{D.1})$$

We define the centered squared increments $dx_t^{2*} = dx_t^2 - \langle dx_t^2 \rangle$.

Their autocorrelation is then

$$\langle dx_t^{2*} dx_{t+\Delta}^{2*} \rangle = \langle dx_t^2 dx_{t+\Delta}^2 \rangle - \langle dx_t^2 \rangle \langle dx_{t+\Delta}^2 \rangle \quad (\text{D.2})$$

$$\begin{aligned} &= 4 \langle D_t D_{t+\Delta} \rangle \left\langle \left(dW_t^{(1)} dW_{t+\Delta}^{(1)} \right)^2 \right\rangle \\ &\quad - 4 \langle D_t \rangle \langle D_{t+\Delta} \rangle \left\langle \left(dW_t^{(1)} \right)^2 \right\rangle \left\langle \left(dW_{t+\Delta}^{(1)} \right)^2 \right\rangle. \end{aligned} \quad (\text{D.3})$$

For $\Delta = 0$, we calculate

$$\langle (dx_t^{2*})^2 \rangle = 12 \langle D_t^2 \rangle - 4 \langle D_t \rangle^2, \quad (\text{D.4})$$

which is obtained directly from Eq. (D.1):

$$\begin{aligned} \langle (dx_t^{2*})^2 \rangle &= 12 \left[\sigma^2 \bar{D} \tau (1 - e^{-t/\tau})^2 + 2\sigma^2 \tau D_0 (e^{-t/\tau} - e^{-2t/\tau}) \right] \\ &\quad + 8 (D_0 e^{-t/\tau} + \bar{D} (1 - e^{-t/\tau}))^2. \end{aligned} \quad (\text{D.5})$$

In the case $\Delta > 0$, as $dW_t^{(1)}$ is independent from $dW_{t+\Delta}^{(1)}$, one has $\left\langle \left(dW_t^{(1)} dW_{t+\Delta}^{(1)} \right)^2 \right\rangle = \left\langle \left(dW_t^{(1)} \right)^2 \right\rangle \left\langle \left(dW_{t+\Delta}^{(1)} \right)^2 \right\rangle$ which leads to

$$\langle dx_t^{2*} dx_{t+\Delta}^{2*} \rangle = 4 \langle D_t D_{t+\Delta} \rangle - 4 \langle D_t \rangle \langle D_{t+\Delta} \rangle. \quad (\text{D.6})$$

The autocorrelation of squared increments is explicitly related to the autocorrelation of diffusivity as

$$\langle dx_t^{2*} dx_{t+\Delta}^{2*} \rangle = 4e^{-(2t+\Delta)/\tau} \int_0^t \int_0^{t+\Delta} e^{(s_1+s_2)/\tau} \langle \sqrt{D_{s_1} D_{s_2}} \rangle \langle dW_{s_1}^{(2)} dW_{s_2}^{(2)} \rangle, \quad (\text{D.7})$$

from which

$$\langle dx_t^{2*} dx_{t+\Delta}^{2*} \rangle = 4e^{-\Delta/\tau} \left[\sigma^2 \bar{D} \tau (1 - e^{-t/\tau})^2 + 2\sigma^2 \tau D_0 (e^{-t/\tau} - e^{-2t/\tau}) \right]. \quad (\text{D.8})$$

Appendix E. Asymptotic analysis at large x

We investigate the asymptotic behavior of the propagator at large x . Let us first consider the particular case $\nu = 1$. As the propagator $P(x, t|x_0)$ is obtained as the inverse Fourier transform of $\tilde{P}(q, t)$, it is instructive to search for the poles of $\tilde{P}(q, t)$ in the complex plane of q in order to compute the inverse Fourier transform by the residue theorem.

We write

$$\tilde{P}(q, t) = \frac{\omega e^{t^*/2}}{f_+(\omega) f_-(\omega)}, \quad (\text{E.1})$$

where

$$f_+(\omega) = \omega \cosh(t^* \omega / 4) + \sinh(t^* \omega / 4), \quad (\text{E.2})$$

$$f_-(\omega) = \omega \sinh(t^* \omega / 4) + \cosh(t^* \omega / 4). \quad (\text{E.3})$$

Setting $\omega = i4\alpha/t^*$, we search for α at which these functions vanish, i.e.,

$$f_+(\omega) = i(4\alpha/t^*) \cos(\alpha) + \sin(\alpha) = 0, \quad (\text{E.4})$$

$$f_-(\omega) = -(4\alpha/t^*) \sin(\alpha) + \cos(\alpha) = 0. \quad (\text{E.5})$$

Both equations have infinitely many solutions. It is easy to see that the solutions of the first equation lie in the intervals $\bigcup_{k=-\infty}^{\infty} (\pi/2 + k\pi, \pi + k\pi)$ (including the trivial solution $\alpha = 0$), whereas the solutions of the second equation lie in the intervals $\bigcup_{k=-\infty}^{\infty} (k\pi, \pi/2 + k\pi)$. Since $\omega = 0$ is not a pole of $\tilde{P}(q, t)$ (as it is compensated by the numerator), we exclude this point. The pole with the smallest absolute value is thus given as the smallest positive solution of the second equation that we rewrite as

$$\alpha_{t^*} \sin \alpha_{t^*} = \frac{t^*}{4} \cos \alpha_{t^*}. \quad (\text{E.6})$$

The smallest positive solution of this equation, α_{t^*} , is a monotonously increasing function of t^* , ranging from 0 at $t^* = 0$ to $\pi/2$ at $t^* = \infty$. The corresponding value of ω will determine the asymptotic exponential decay of the propagator.

Since $i4\alpha_{t^*}/t^* = \omega = \sqrt{1 + 4q^2\sigma^2\tau^2}$, we identify the pole in the q plane:

$$q_0 = \pm i\beta_{t^*} \frac{1}{2\sigma\tau}, \quad \beta_{t^*} = \sqrt{1 + (4\alpha_{t^*}/t^*)^2}. \quad (\text{E.7})$$

Applying the residue theorem, we get

$$P(x, t|x_0) = \int_{-\infty}^{\infty} \frac{dq}{2\pi} e^{iq(x-x_0)} \tilde{P}(q, t) = 2\pi i \sum_n \frac{e^{iq_n(x-x_0)}}{2\pi} \text{res}_{q_n} \{ \tilde{P}(q, t) \}, \quad (\text{E.8})$$

where the sum runs over the poles. The asymptotic behavior at large $|x - x_0|$ is determined by the pole with the smallest $|q_0|$. We get thus Eq. (21). One can also compute the prefactor by evaluating the residue of $\tilde{P}(q, t)$ at $q = q_0$. Note that for large t^* , one has $\alpha_{t^*} \approx \pi/2$, and thus the dependence on t^* is eliminated, yielding $\beta_{t^*} \simeq 1$ as $t^* \rightarrow \infty$. In turn, when t^* is small, one has $\alpha_{t^*} \simeq \sqrt{t^*}/2$, and thus $\beta_{t^*} \simeq \sqrt{1 + 4/t^*} \rightarrow \infty$. As a consequence, the distribution becomes more and more narrowed, as expected. We emphasize that this analysis is not rigorous enough, as the relation between q and ω involves the square root and thus requires some cuts in the complex plane to avoid multiple branches.

When ν is a strictly positive integer, the above analysis remains applicable. However, the pole is not simple (as for $\nu = 1$) but has a degree ν . The degree $\nu > 1$ results in a more complicated computation of the residue and, more importantly, in power law corrections to the exponential decay in Eq. (23).

We also emphasize that the current analysis only focuses on the dependence on $|x - x_0|$ and does not capture the complete dependence on t^* which enters through different coefficients.

[1] Weiss M, Elsner M, Kartberg F, and Nilsson T, 2004, *Biophys. J.*, **87**, 351824.

[2] Barkai E, Garini Y, and Metzler R, 2012, *Phys. Today*, **65**, 2935.

- [3] Höfling F and Franosch T, 2013, *Rep. Prog. Phys.*, **76**, 046602.
- [4] Manzo C, Torreno-Pina J A, Massignan P, Lapeyre G J, Lewenstein M, and Garcia Parajo M F, 2015 *Phys. Rev. X*, **5**, 14.
- [5] Sadegh S, Higgins J L, Mannion P C, Tamkun M M, and Krapf D, 2017, *Phys. Rev. X*, **7**, 11031.
- [6] Havlin S and Ben-Avraham D, 2002, *Adv. Phys.*, **36**, 187-292.
- [7] Metzler R, Jeon J H, Cherstvy A G, and Barkai E, 2014, *Phys. Chem. Chem. Phys.*, **16**, 24128-24164.
- [8] Spanner M, Höfling F, Kapfer S C, Mecke K R, Schröder-Turk G E, and Franosch T, 2016, *Phys. Rev. Lett.*, **116**, 060601.
- [9] Mandelbrot B B, Van Ness J W, 1968, *SIAM Rev.*, **10**, 4.
- [10] Wang K G, 1992, *Phys. Rev. A*, **45**, 833.
- [11] Porrá J M, Wang K G, Masoliver J, 1996, *Phys. Rev. E*, **53**, 5872.
- [12] Grebenkov D G, 2011, *Phys. Rev. E* **83**, 061117.
- [13] Montroll E W and Weiss G H, 1965, *J. Math. Phys.*, **6**, 167.
- [14] Metzler R and Klafter J, 2000, *Phys. Rep.*, **339**, 1-77.
- [15] Orpe A V and Kudrolli A, 2007, *Phys. Rev. Lett.*, **98**, 238001.
- [16] Gollub J P, Clarke J, Gharib M, Lane B, and Mesquita O N, 1991, *Phys. Rev. Lett.*, **67**, 3507-3510.
- [17] Stuhrmann B, Soares E Silva M, Depken M, MacKintosh F C and Koenderink G H, 2012, *Phys. Rev. E*, **86**, 15.
- [18] Toyota T, Head D A, Schmidt C F and Mizuno D, 2011, *Soft Matter*, **7**, 3234.
- [19] Bertrand O J N, Fygenon D K and Saleh O A, 2012, *Proc. Natl. Acad. Sci. USA*, **109**, 17342-17347.
- [20] Moschakis T, Lazaridou A and Biliaderis C G, 2012, *J. Coll. Inter. Sci.*, **375**, 5059.
- [21] Chaudhuri P, Berthier L and Kob W, 2007, *Phys. Rev. Lett.*, **99**, 060604.
- [22] Grady M E, Parrish E, Caporizzo M A, Seeger S C, Composto R J, Eckmann D M, 2017, *Soft Matter*, **13**, 1873-1880.
- [23] Wang B, Anthony S M, Bae S C and Granick S, 2009, *Proc. Nat. Acad. Sci.*, **106**, 15160-15164.
- [24] Wang B, Kuo J, Bae S C and Granick S, 2012 *Nat. Mater.* **11**, 481-485.
- [25] Drăgulescu A A and Yakovenko V M, 2011, *Quant. Fin.*, **2**, 443-453.
- [26] Rouyer F and Menon N, 2000, *Phys. Rev. Lett.*, **85**, 3676-3679.
- [27] He W, Song H, Su Y, Geng L, Ackerson B J, Peng H B and Tong P, 2016, *Nat. Com.*, **7**, 11701.
- [28] Ghosh S K, Cherstvy A G and Metzler R, 2015, *Phys. Chem. Chem. Phys.*, **17** 1847.
- [29] Ghosh S K, Cherstvy A G, Grebenkov D S and Metzler R, 2016, *New. J. Phys.*, **18**, 013027.
- [30] Metzler R, 2017, *Biophys. J.*, **112**, 413-447.
- [31] Kärger J, 1985, *Adv. Coll. Int. Sci.*, **23**, 129-148.
- [32] Fieremans E, Novikov D S, Jensen J H, Helpert J A, 2010, *NMR Biomed.* **23**, 711-724.
- [33] Chubynsky M V and Slater G W, 2014, *Phys. Rev. Lett.*, **113**, 098302.
- [34] Beck C and Cohen E G D, 2003, *Physica A*, **322**, 267-275.
- [35] Beck C, Cohen E G D, and Swinney HL, *Phys. Rev. E*, **72**, 056133.
- [36] Jain R and Sebastian K L, 2016, *J. Phys. Chem. B*, **120**, 3988-3992.
- [37] Jain R and Sebastian K L, 2017, *J. Chem. Sci.*, **126**, 929-937.
- [38] Jain R and Sebastian K L, 2017, *Phys. Rev. E*, **95**, 032135.
- [39] Chechkin A V, Seno F, Metzler R, and Sokolov I M, 2017, *Phys. Rev. X*, **7**, 021002.
- [40] Higham D J, 2001, *SIAM Rev.*, **43**, 525-546.
- [41] Cox J C, Ingersoll J E, Ross S A, 1985, *Econometrica*, **53**, 385-408.
- [42] Heston S L, 1993, *Rev. Fin. Studies.*, **6**, 327-343.
- [43] Chen L, 1996, *Financial Markets, Institutions and Instruments.*, **5**, 1-88.
- [44] He Y, Burov S, Metzler R and Barkai E, 2008, *Phys. Rev. Lett.*, **101**, 058101.
- [45] Burov S, Jeon J H, Metzler R, and Barkai E, 2010, *Phys. Chem. Chem. Phys.*, **13**, 1800-1812.
- [46] Schwarzl M, Godec A, and Metzler R, 2017, *Sci. Rep.*, **7**, 3878.
- [47] Grebenkov D S, 2011, *Phys. Rev. E*, **84**, 031124.

- [48] Sikora G, Teuerle M, Wyomaska A, and Grebenkov D S, 2017, *Phys. Rev. E*, **96**, 022132.
- [49] Qian H, Sheetz M P, Elson E L, 1991, *Biophys. J.*, **60**, 910-921.
- [50] Cherstvy A G and Metzler R, 2016, *Phys. Chem. Chem. Phys.*, **18**, 23840-23852.
- [51] Kindermann F, Dechant A, Hohmann M, Lausch T, Mayer D, Schmidt F, Lutz E and Widera L, 2016, *Nat. Phys.*, **13**, 137-141.
- [52] Magdziarz M and Weron A, 2011, *Phys. Rev. E*, **84**, 051138.
- [53] Lanoiselée Y and Grebenkov D S, 2016, *Phys. Rev. E*, **93**, 052146.
- [54] Jensen J H, Helpert J A, Ramani A, Lu H, Kaczynski K, 2005, *Magn. Reson. Med.*, **53**, 1432-1440.
- [55] McCauley J J, 2013, *Cambridge University Press*.
- [56] Feller W, 1951, *Ann. Math.* **54**, 173-182.
- [57] Weron A and Magdziarz M, 2009, *Eur. Phys. Lett.*, **86**, 60010.
- [58] Thiel F, Flegel F, and Sokolov I M, 2013, *Phys. Rev. Lett.*, **111**, 010601.
- [59] Dufresne D, 2001, *Working Paper, University of Melbourne*.